Molecular Vision 2019; 25:266-282 <http://www.molvis.org/molvis/v25/266>
Received 3 January 2019 | Accepted 25 April 2019 | Published 27 April 2019

Analysis of interleukin-20 receptor complexes in trabecular meshwork cells and effects of cytokine signaling in anterior segment perfusion culture

Kate E. Keller,[1] Yong-feng Yang,[1] Ying Ying Sun,[1] Mark R. Walter,[2] Mary K. Wirtz[1]

[1]Department of Ophthalmology, Oregon Health & Sciences University, Portland, OR; [2]Department of Microbiology, University of Alabama at Birmingham, Birmingham, AL

Purpose: Inflammatory responses may be involved in the glaucomatous process. Our previous studies mapped a T104M mutation in interleukin-20 receptor beta (*IL-20RB*) in a family with primary open angle glaucoma (POAG). IL-20RB can heterodimerize with IL-20RA to propagate signals from IL-20 family cytokines, IL-19, IL-20, and IL-24 (the type I receptor complex), or it can heterodimerize with IL-22RA to propagate signals from IL-20 and IL-24 (type II receptor complex). In this study, we investigated IL-20 heterodimeric receptor complexes in the trabecular meshwork (TM) compared to dermal fibroblast cell cultures, and examined the phosphorylation of signal transducer and activator of transcription (STAT)-1, -3, and -5 following exposure to IL-20 family cytokines. Additionally, we determined the effects of IL-20 family cytokines on outflow rates in anterior segment perfusion culture, an in vitro model of intraocular pressure (IOP) regulation.

Methods: Primary human TM (HTM) cells were grown from dissected TM tissue, and IL-20 receptor expression was investigated with PCR. A Duolink assay was performed to investigate in situ IL-20 receptor protein interactions in HTM or dermal fibroblasts, and Imaris software was used to quantitate the association of the heterodimeric complexes. Phosphorylation of STAT-1, -3, and -5 were evaluated in HTM or dermal fibroblasts using Western immunoblotting after exposure to IL-10, IL-19, IL-20, IL-22, or IL-24. Anterior segment perfusion culture was performed in human cadaver and porcine eyes treated with IL-20, IL-19, or IL-24.

Results: All of the IL-20 receptors, IL-20RA, IL-20RB, and IL-22RA1 were expressed in HTM cells. Two isoforms of IL-20RA were expressed: The V1 variant, which is the longest, is the predominant isoform, while the V3 isoform, which lacks exon 3, was also expressed. The Duolink assay demonstrated that the type I (IL-20RA–IL-20RB) and type II (IL-22RA1–IL-20RB) receptors were expressed in HTM cells and dermal fibroblasts. However, in the HTM cells, the type I receptor was present at significantly higher levels, while the type II receptor was preferentially used in the dermal fibroblasts. The HTM cells and the dermal fibroblasts predominantly phosphorylate the Ser727 site in STAT-3. The dermal fibroblasts had higher induction of phosphorylated STAT-1 compared to the HTM cells, while neither cell type had phosphorylated STAT-5 in the cell lysates. The outflow rates in the human anterior segment cultures were increased 2.3-fold by IL-20. However, IL-19 and IL-24 showed differential responses. For IL-19 and IL-24, 50% of the eyes responded with a 1.7- or 1.5-fold increase, respectively, while the other half did not respond. Similarly, perfused porcine anterior segments showed “responders” and “non-responders”: IL-20 responders (2.3-fold increase in outflow, n=12) and non-responders (n=11); IL-19 responders (2.1-fold increase, n=7) and non-responders (n=5); and IL-24 responders (1.8-fold increase, n=12) and non-responders (n=5).

Conclusions: Type I and type II IL-20 receptor complexes are expressed in human TM cells with predominant expression of the type I receptor (IL-20RA and IL-20RB), which propagates signals from all three IL-20 family cytokines. However, there was a variable response in the outflow rates following perfusion of cytokines in two different species. This may explain why some people are more susceptible to developing elevated IOP in response to inflammation.

Glaucoma is a group of diseases resulting from damage to the optic nerve that leads to a distinctive pattern of vision loss. Nearly 112 million individuals will develop glaucoma by 2040, making glaucoma the leading cause of global irreversible blindness [1]. Primary open angle glaucoma (POAG) is the most common form of glaucoma in Western and African nations [1]. Because the symptoms are subtle in the early stages of the disease, many individuals remain undiagnosed until severe visual field loss has occurred. Vision loss from glaucoma has a significant impact on health-related quality of life, and the overall burden increases as glaucomatous damage and vision loss progress [2]. The exact etiology of POAG remains unknown, although it is clear that it is a heterogeneous group of disorders and is frequently associated with elevated intraocular pressure (IOP) [3-5]. Although lowering IOP often reduces the rate of vision loss, many

Correspondence to: Mary K. Wirtz, Department of Ophthalmology, Oregon Health & Sciences University, Portland, OR 97239 Phone: (503) 494 4698; email: wirtzm@ohsu.edu

patients continue to go blind despite apparently "successful" pressure control [4-6]. Elevated IOP is caused by dysfunction of the aqueous humor drainage pathway in the trabecular meshwork (TM) tissue in the anterior of the eye [7], which eventually damages optic nerve axons, resulting in retinal ganglion cell death and visual impairment [8-10].

There are potentially many disease mechanisms behind glaucoma. Recent studies suggested that inflammatory responses may be involved in the glaucomatous process, as shown by human studies and in rodent models [11-15]. Drugs such as glucocorticoids are often used to treat inflammatory and autoimmune disease, but in certain individuals, these drugs can have serious side effects, such as the development of ocular hypertension and glaucoma [16-18]. Becker and Mills found that normal patients fell into two distinct subgroups: those exhibiting a moderate increase in IOP and those exhibiting no increase in IOP [19]. Follow-up studies refined the characterization of response to glucocorticoids in normal patients, recognizing three distinct subgroups: those exhibiting a high response (a change >15 mmHg), those exhibiting a moderate response (a change of 6–15 mmHg), and those exhibiting a low response (a change <6 mmHg) [20,21]. Subsequently, individuals with a predisposition to develop elevated IOP when treated with glucocorticoids systemically or locally in the eye were referred to as "steroid responders," a term coined by Armaly and Becker [20].

Other studies have demonstrated a genetic component of glaucoma [22-26]. In 1997, our group mapped the *GLC1C* (Gene ID 50604; OMIM 601682) locus in a large family with POAG to a region on chromosome 3 [23]. Subsequently, a T104M mutation in the *interleukin-20 receptor beta* (*IL-20RB*; Gene ID 50604; OMIM 605621) gene was identified in 11 members of this family who had POAG [11]. All 11 individuals have high IOPs ranging from 22 to 46 mmHg [11]. The T104M mutation identified in the family with POAG is located in the IL-20/IL-20RB binding interface [27]. Therefore, it is likely that patients with glaucoma with this mutation cannot respond appropriately to cytokine signaling, leading to an inadequate homeostatic response to elevated IOP. IL-20 family cytokines (IL-19, IL-20, and IL-24) and receptors (IL-20RA, IL-20RB, IL-22RA1) are members of the larger IL-10 family, which were grouped together based on conserved receptor sequences [28]. IL-19 signals exclusively through the type I receptor, a heterodimer consisting of IL-20RA and IL-20RB (Figure 1) [27]. IL-20 and IL-24 can signal through either the type I receptor or the type II receptor, which is composed of IL-22RA1 and IL-20RB [27,28]. IL-22 and IL-26 do not signal through IL-20RB, but instead use heterodimeric complexes consisting of IL-22RA1/IL-10RB, and IL-20RA/IL-10RB, respectively [28].

The IL-20 family has been proposed to have proinflammatory, angiogenic, and chemoattractive effects on chronic inflammatory diseases, including psoriasis, atherosclerosis, and rheumatoid arthritis [29,30]. This family of cytokines enhances tissue remodeling and wound-healing activities, maintaining tissue integrity and restoring homeostasis of the epithelial layers during infection and inflammatory responses [31]. Interestingly, IL-24 was first reported as an antitumor molecule, and was originally named melanoma differentiation-associated 7 (mda-7) [32]. The IL-20 family is known to be expressed in myeloid, epithelial, and T cells, as well as innate lymphoid cells. However, little is known about IL-20 family signaling in the TM [28].

Our previous genetic study reported a T104M mutation in the extracellular domain of the IL-20RB in a family with glaucoma, but it remains unclear which IL-20 receptors are expressed in normal TM cells, and whether the IL-20 receptor complexes are functional. The purpose of this study was to investigate expression of IL- 20 heterodimeric receptor complexes in TM cell cultures, and to measure the effects of IL-20 family cytokines on outflow rates in anterior segment perfusion culture, an in vitro model of IOP regulation.

METHODS

Cell culture: Human TM (HTM) cells were grown from TM tissue from cadaver eyes (Lions VisionGift, Portland, OR) or from corneal rims discarded following corneal transplant surgery (Casey Eye Institute, Portland, OR) [33]. A summary of the donors for the cell strains used in this manuscript is included in Appendix 1. HTM cells were grown in a 1:1 mixture of high and low glucose Dulbecco's modified Eagle's medium (DMEM) containing 10% fetal bovine serum (FBS; Fisher Scientific, Waltham, MA) and 1% penicillin-streptomycin-Fungizone (Gibco, Waltham, MA). HTM cell cultures were split 1:3, and used up to passage 6. All TM cell cultures were examined morphologically and tested for their ability to induce myocilin protein after exposure to dexamethasone for 2 weeks, the current standard for characterizing primary TM cells [33]. Adult human dermal fibroblasts were purchased from three commercial sources: PromoCell (age: 60, sex: male, cell source: cheek skin; Heidelberg, Germany), MilliporeSigma (age: 38, sex: female; cell source: abdominal skin; St. Louis, MO), and ATCC (age: 50, sex: female, cell source: abdominal skin; Manassas, VA). All fibroblasts were maintained in DMEM containing 10% FBS and 1% penicillin-streptomycin-Fungizone.

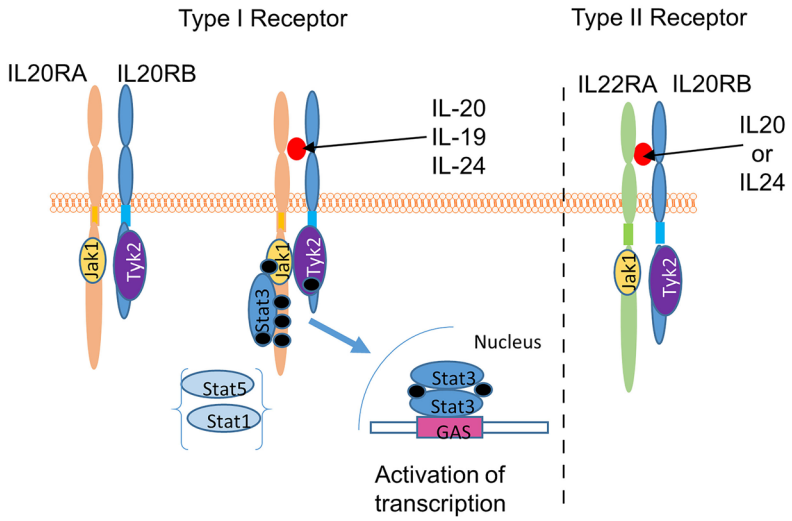

Figure 1. Schematic of interleukin-20 receptor complex before and after activation by IL-20, -19, or -24. The type I receptor is composed of the interleukin-20RA (IL-20RA) and IL-20RB proteins while the type II receptor contains the IL-22RA1 and IL-20RB proteins [28,30,61]. Upon cytokine binding, Jak1 binds near the transmembrane region of IL-20RA and IL-22RA1. Tyk2 is proposed to bind to IL-20RB based on sequence homology between IL-20RB and interferon-γ receptor 1 (IFNγR1) [62]. Binding of the cytokine results in closer juxtaposition of Jak1 and Tyk2, leading to autophosphorylation of the tyrosine kinases, phosphorylation of IL-20RA, and recruitment and phosphorylation of signal transducer and activator of transcription (STAT)-3, STAT-1, and possibly, STAT-5 [61,63]. The STATs can then translocate to the nucleus to activate transcription.

IL-20 receptor PCR: HTM cells (n=5) or human dermal fibroblasts were grown until confluent. RNA was isolated in TRIzol (ThermoFisher, Grand Island, NY) and purified with the Direct-zol RNA miniprep kit (Zymo Research, Irvine, CA). Total RNA concentration and purity were quantitated with a NanoDrop 2000 (Wilmington, DE). Superscript III reverse transcriptase (ThermoFisher) was used to generate cDNA using 300–600 ng RNA as a template. PCR products were amplified (94 ºC for 15 min, then 32 cycles of 94 ºC for 30 s, 60 ºC for 30 s and 72 ºC for 45 s, followed by a final extension of 72 ºC for 10 min) on a thermal cycler using the primers listed in Appendix 2. To investigate the alternative splicing of IL-20RA, primers (602S and 603AS) were designed to flank exon 3, and reverse transcriptase (RT)–PCR was performed. Products were separated on an agarose gel and purified, and DNA sequencing was performed to confirm the identity of the products.

Duolink assay: To investigate IL-20 receptor protein interactions in cells, an in situ Duolink proximity ligation assay (PLA; Duolink Red starter kit for mouse and goat; Millipore-Sigma) was performed. This assay uses primary antibodies to each receptor subunit, which were raised in different host species, and detected with secondary antibodies conjugated to PLA probes. When the two primary antibodies are in close proximity (<40 nm), the DNA strands on the probes are joined by ligation into a circular DNA molecule, which is then amplified with “rolling-circle amplification” (RCA) primed by one of the probes. The RCA product was detected with hybridization of fluorescently labeled oligonucleotides. HTM or human dermal fibroblasts were grown to approximately 70% confluence and then fixed in 4% paraformaldehyde. The assay was then performed following the manufacturer’s instructions: Briefly, after blocking at 37 °C for 1 h, the cells were incubated with primary antibody overnight at 4 °C. Antibody combinations were IL-20RB (goat polyclonal; R&D Systems, Minneapolis, MN) and IL-20RA (Mouse monoclonal; R&D Systems), or IL-20RB and IL-22RA1 (mouse monoclonal; R&D Systems). Negative controls were performed by substituting the primary antibody with PBS (1X; 155 mM NaCl, 3 mM Na_2HPO_4, 1 mM KH_2PO_4, pH 7.4; Gibco, Waltham, MA) After washing, the primary antibodies were incubated with the PLA probes, which were subsequently ligated with incubation with ligase. Signals were amplified by the addition of polymerase for 1 h 40 min at 37 °C. After final washes, coverslips were mounted in mounting medium containing 4′,6-diamidino-2-phenylindole (DAPI). Confocal z-stack images were acquired with confocal microscopy (Olympus Fluoview, Center Valley, PA), and the number of punctate dots and nuclei per field were counted using the “spots” module of Imaris software (Bitplane, Concord, MA). Results are reported as the number of spots/nuclei in a field, and seven to 14 fields were counted for each receptor type in each cell type, and then averaged. Data were analyzed with one-way ANOVA to determine significance with Bonferroni correction. A p value of less than 0.025 was considered statistically significant.

Western immunoblotting: HTM cells or dermal fibroblasts were grown to confluence in DMEM + 10% FCS, washed with PBS, and placed in serum-free media overnight. The next day, the serum-free media were replaced, and the following recombinant human cytokines were added for 15 min: IL-10, IL-19, IL-20, IL-22, or IL-24 (all 100 ng/ml; R&D Systems). An untreated control was also included. Cell lysates were harvested in RIPA buffer, and the proteins were separated on 10% sodium dodecyl sulfate–polyacrylamide gel electrophoresis (SDS–PAGE) gels and transferred to nitrocellulose membranes. The membranes were then probed with the following signal transducer and activator of transcription (STAT) antibodies (all antibodies from Cell Signaling Technology Inc., Danvers, MA, unless stated otherwise): phospho-tyrosine701 STAT-1 (mouse monoclonal; ThermoFisher, 33–3400), total STAT-3 (mouse monoclonal; 9139), phospho-serine727 STAT-3 (rabbit polyclonal; 9134), phospho-serine705 STAT-3 (rabbit polyclonal; 9131), total STAT-5 (rabbit polyclonal; 25,656), and phospho-TyrosineY694 (mouse monoclonal; 9356). After washing and incubation with infrared (IR)-dye-conjugated secondary antibodies, the membranes were imaged on the Li-Cor Odyssey (Lincoln, NE) imaging system. Densitometry was used to measure band intensity using FIJI software (provided in the public domain). Experiments were performed at least three times using at least three biologic replicates for each cell type. Data from each experimental replicate (n=3–6) were normalized to the total STAT-3 loading control, made a percentage of the untreated control. Then, the data were averaged for each treatment, and a standard error of the mean calculated. Statistical significance was set at a p value of less than 0.05.

Anterior segment perfusion culture: Human cadaver eyes were acquired from the Lions VisionGift eye bank. Information on donor eyes can be found in Appendix 1. The eye globes were bisected, and the lens, ciliary body, and iris were removed from the anterior segment. After dissection, the human anterior segments were maintained in serum-free stationary organ cultures to allow recovery of the cells postmortem. Porcine eyes were acquired from a local abattoir (Carlton Farms, Carlton, OR), and dissected within 4 h of death. For both species, anterior segment containing the cornea, trabecular meshwork, and sclera was clamped into a perfusion chamber and perfused with serum-free DMEM at a constant pressure of 8 mmHg [34]. After 24 h, any anterior segment that was not stabilized at a flow rate of 1–8 µl/min was discarded [35]. Flow rates were measured for 4 h before 100 ng/ml of human recombinant IL-20, IL-19 or IL-24 (R&D Systems, Minneapolis, MN) were added in 100 µl of PBS to the intake port. Perfusion was resumed for a further 70–73 h, and the flow rates were measured. For each eye, the flow rates after treatment were normalized to the average flow rate before the cytokines were added. Individual eye data were combined and averaged, and a standard error of the mean calculated. Statistical significance was determined using a one-way ANOVA, where a p value of less than 0.05 was considered statistically significant.

Structure alignment of human and porcine sequences: Amino acid sequences of human and porcine IL-20 receptors were obtained from the NCBI. The sequences were aligned using Clustal Omega [36]. Residues involved in IL-20–IL-20RA, IL-20–IL-20RB, IL-20RA–IL-20RB, and IL-22–IL-22RA1 interactions were identified using the crystal structures of the IL-20–IL-20RA–IL-20RB complex (pdbid 4doh) and the IL-22–IL-22RA1 complex (pdbid 3dgc). Contact residues that bury surface area in the interfaces were identified using the PISA server [37] and validated with computer graphics using the program pymol.

RESULTS

In this study, we investigated IL-20 receptor family expression in human TM cells and dermal fibroblasts. With RT–PCR, all of the IL-20 receptors, IL-20RA, IL-20RB, and IL-22RA1 were expressed in human TM cells, as well as the related receptor, IL-10RB (Figure 2A). Four alternatively spliced isoforms of IL-20RA are reported in the NCBI database (V1: NM_014432.2), V2: NM_001278722.1, V3: NM_001278723.1, and V4: NM_001278724.1), which vary in the untranslated region (UTR) and extracellular binding region of the receptor. Therefore, we investigated which splice forms are expressed by HTM cells and dermal fibroblasts. In both cell types, the longest V1 variant was the predominant isoform expressed, but the V3 isoform, which lacks exon 3 encoding an extracellular domain, was also expressed (Figure 2B). Using appropriate primer sets, we did not detect isoforms V2 or V4 in either the HTM cells or the dermal fibroblasts (data not shown).

Next, we investigated which receptor complex, that is, the type I receptor (IL-20RA–IL-20RB heterodimer) or the type II receptor (IL-22RA1–IL-20RB heterodimer), was used in dermal fibroblasts and HTM cells. We used the in situ Duolink proximity ligation assay, which investigates protein interactions in fixed cells [38]. In this assay, IL-20 receptor heterodimers were visualized as punctate dots with confocal microscopy (Figure 3A–D). The type I and type II receptors were identified in both cell types. However, after quantification of the number of dots, there was a statistically significant difference between the type I and type II receptors in the fibroblasts compared to the HTM cells. In the dermal fibroblasts, there were statistically significantly more dots detected

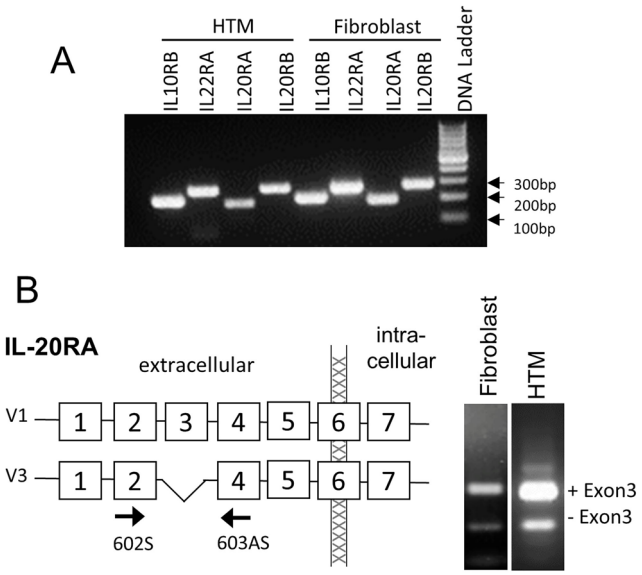

Figure 2. IL-20 receptor family member expression. **A**: PCR shows the mRNA expression of interleukin-20RA (IL-20RA), IL-20RB, IL-22RA1, and IL-10RB in human dermal fibroblasts and human trabecular meshwork (HTM) cells. **B**: Analysis of IL-20RA alternative splicing in dermal fibroblasts and HTM cells. Full-length variant 1 (V1) and variant 3 (V3), which lacks exon 3, were detected in both cell types.

with the IL-20RB and IL-22RA1 antibodies, whereas in the HTM cells, there were statistically significantly more dots detected with the IL-20RB and IL-20RA antibody pairings (Figure 3E). A negative control where primary antibodies were replaced by PBS is shown (Appendix 3). This suggests that HTM primarily signal via type I receptors, while dermal fibroblasts prefer type II receptors.

Once IL-20 family cytokines bind to the heterodimeric IL-20 receptor complexes, STATs become activated (Figure 1). The potential for STAT activation is based on the finding that IL-22 induces STAT-1, -3, and -5 through the IL-22RA1/IL-10RB complex in hepatoma cells [39]. However, it is unknown which STATs are used in TM cells. Therefore, we investigated STAT phosphorylation in the HTM cells compared to the dermal fibroblasts (Figure 4). STAT-1 is phosphorylated at Tyr701 [40]. In the HTM cells, there were lower levels of phosphorylated STAT-1 in cell lysates compared to the levels in the dermal fibroblasts. Although all cytokines, and IL-22 in particular, induced Tyr701 STAT-1 phosphorylation in the dermal fibroblasts, there was no such induction by IL-22, or any of the cytokines, in the HTM cells. The major two phosphorylation sites of STAT-3 are Ser727 and Tyr705 [41]. The present results showed that the HTM cells and dermal fibroblasts predominantly phosphorylate STAT-3 on the Ser727 site. The phospho-Ser727 antibody detected two bands in the serum-free controls, but there was a marked shift to the upper band after 15 min. In the HTM cells, the upper band was increased compared to that in the serum-free controls, which suggests activation via this phosphorylation site. Densitometry was used to quantitate Ser727 phosphorylation of STAT-3 (Figure 4C). In the HTM cells (n=6), all the cytokines tested induced phosphorylation of Ser727. However, in the dermal fibroblasts (n=3), IL-20, IL-22, and IL-24 induced phosphorylation, whereas IL-10 and IL-19 did not. The STAT-3 Tyr705 phosphorylation site was not used, apart from when the dermal fibroblasts were stimulated with IL-22. STAT-5 is phosphorylated at Tyr694 [42]. Much lower amounts of STAT-5 were detected in lysates from both cell types compared to STAT-3, and none of the cytokines stimulated phosphorylation of Tyr694 in either cell type. Thus, the IL-20 family cytokines appear to predominantly signal via phosphorylation of STAT-3 at the Ser727 site in HTM cells.

Anterior segment perfusion culture is a standard ex vivo technique for measuring the effects of agents on the outflow rates through the TM [34,35,43-45]. The T104M mutation in IL-20RB found in patients with POAG suggests that it may disrupt signaling from IL-20, IL-19, or IL-24, but not from IL-10, IL-22, or IL-26. Therefore, we tested the impact of IL-20, IL-19, and IL-24 signaling on the outflow rates using human (Figure 5) and porcine anterior segments (Figure 6). For human eyes, data from three eyes were discarded as the initial flow rates were below 1 µl/min. Application of IL-20 to human anterior segments (n=7) caused an average flow rate increase of 2.3-fold, in all eyes tested, over the 70 h experiment, compared to the vehicle control (Figure 5A). However, application of IL-19 or IL-24 had variable effects. Fifty percent of eyes tested showed increased flow rates (responders) while an equal number showed no effect (non-responders). Non-responders were defined as having a flow

rate that did not go above 1.2 µl/min, while responders had flow rates >1.23 µl/min. For eyes that responded, the fold increase was lower than in the IL-20 treatment: IL-19 induced a 1.7-fold increase (Figure 5B), while IL-24 caused a 1.5-fold increase over 70 h (Figure 5C). Raw flow rate data for human eyes are shown in Table 1.

To further investigate the effects of these cytokines on outflow, we used porcine eyes, because they are more readily available. In perfused porcine anterior segments (Figure 6), there were responders and non-responders with all three cytokine treatments. For IL-20, 12 anterior segments increased the outflow to approximately 2.1-fold, whereas 11 anterior segments did not respond (Figure 6A). One outlier was excluded from the data analysis. For IL-19, seven eyes responded with a 2.1-fold increase in outflow, while five eyes had no response (Figure 6B). For IL-24, 12 eyes responded with a 1.8-fold increase in outflow, while five eyes did not respond (Figure 6C). The raw flow rate data for porcine eyes are shown in Table 2, Table 3, and Table 4. We also analyzed the final flow rate data at the 73 h time point (Figure 7). When we grouped the data together as “responders” versus “non-responders,” a significant difference was observed for each cytokine (Figure 7).

For the porcine eyes, we hypothesized that the human recombinant cytokine may not bind porcine receptors. Therefore, we analyzed the porcine IL-20 receptor protein sequences, and found that all of the residues that make direct contact with the cytokines were conserved (Figure 8) [27]. Thus, human recombinant cytokine should bind effectively to porcine receptors.

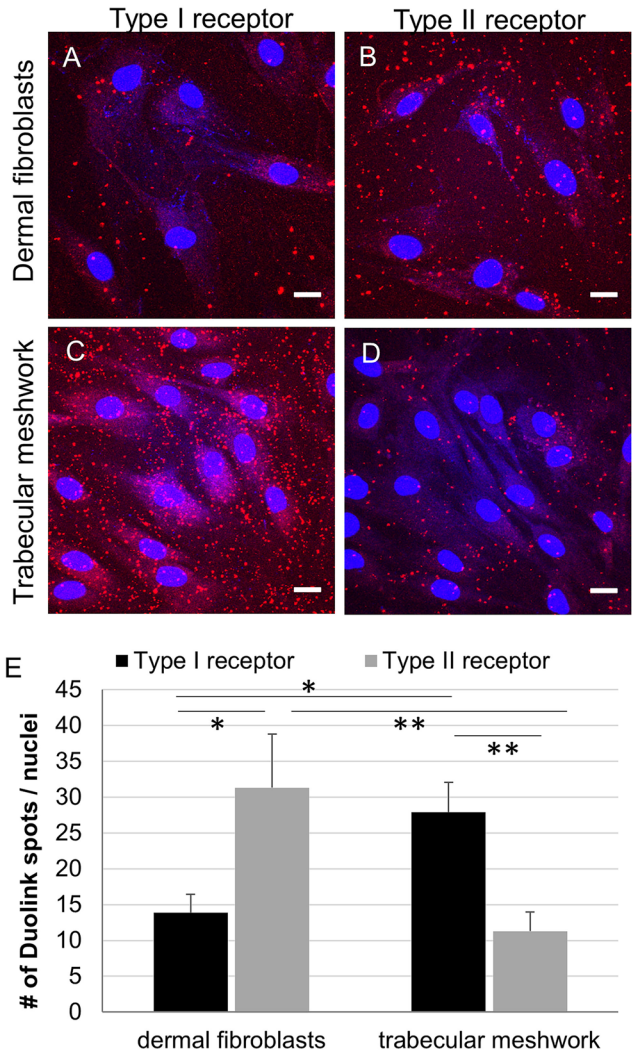

Figure 3. IL-20R in situ protein interactions. Duolink proximity ligation assay confocal images of normal human dermal fibroblasts (**A**, **B**) or human trabecular meshwork (TM) cells (**C**,**D**). Representative images of type I (interleukin-20RA (IL-20RA)–IL-20RB) and type II (IL-22RA1–IL-20RB) receptor complexes are shown. Scale bar = 20 µm. **E**: The number of spots and nuclei was counted with Imaris software in seven to 14 fields for each receptor type in at least four different experiments using three biologic replicates for each cell type. * $p \leq 0.024$ and ** $p < 0.003$ with one-way ANOVA.

DISCUSSION

In this study, we investigated the expression and function of IL-20 receptor complexes in regard to aqueous outflow regulation in the trabecular meshwork, which is dysfunctional in glaucoma [7]. We initially became interested in the IL-20 family cytokines when we discovered a T104M mutation in IL-20RB in a large family with POAG [11]. This mutation is predicted to impact cytokine binding to the IL-20RB chain [27]. The IL-20 cytokine family is unusual, because of the promiscuity of the type I and type II receptors [30]. However, all three ligands (IL-20, IL-19, and IL-24) can signal through the type I receptor (IL-20RA–IL-20RB), while only IL-20 and IL-24 signal through the type II receptor (IL-22RA1–IL-20RB). This raises the question of how specificity is engendered by type I and type II receptors. In this study, we showed that IL-20RA, IL-20RB, IL-22-RA1 and IL-10RB are expressed in TM cells, as well as in skin fibroblasts. Additionally, we showed that the IL-20RA isoforms V1 and V3, which lacks exon 3, are expressed by TM cells and fibroblasts. Exon 3 contains the critical YG (Tyr-76 and Gly-77) interaction motif, as well as Glu105, Tyr-109, and Arg-128, which are involved in the binding of IL-20 cytokines by IL-20RA [27]. Domain 1 is completely absent in the IL-20RA V3 protein. Thus, the V3 isoform may act as a competitive inhibitor reducing the amount of cytokine available to the receptor [27].

Although it appears that HTM cells and dermal fibroblasts express all the IL-20 receptor subunits, each cell type may preferentially use different receptor complexes. The Duolink assay, which measures the colocalization of proteins, showed increased numbers of type-I complexes in the HTM cells. Conversely, in fibroblasts, type II receptor complexes predominated. Thus, the present results suggest that HTM cells can respond to all three cytokines, whereas dermal fibroblasts may preferentially respond to IL-20 and IL-24. This suggestion is supported by the western immunoblot data, where all cytokines induced phosphorylation of Ser727 of STAT-3 in the HTM cells, but IL-19 did not affect

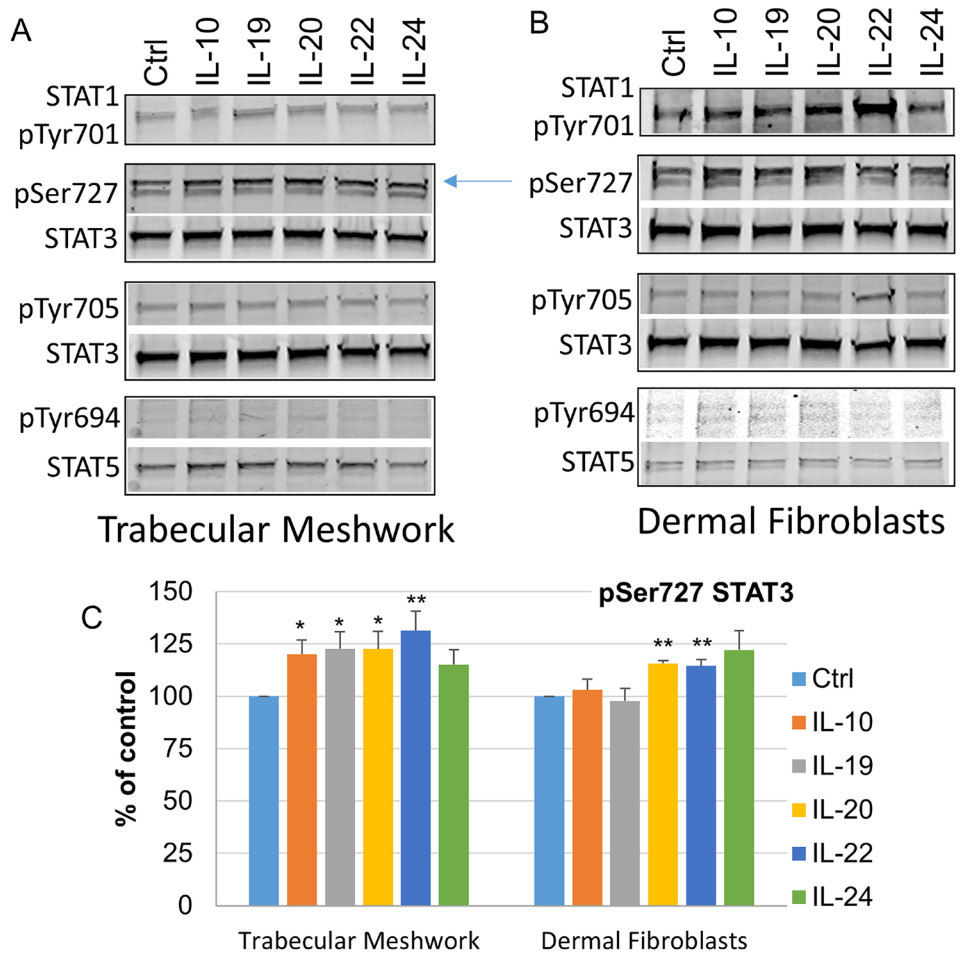

Figure 4. Western immunoblot analysis of STAT phosphorylation. Western immunoblot analysis of signal transducer and activator of transcription (STAT)-1 Tyr701, STAT-3 Ser727, STAT-3 Tyr705, and STAT-5 Tyr694 phosphorylation in (**A**) normal human trabecular meshwork cells or (**B**) normal human dermal fibroblasts treated with the indicated interleukins for 15 min. Total STATs were used as loading controls. The arrow points to the upper phosphorylated band. C: Densitometry of the phosphorylated Ser727 STAT-3 band. Trabecular meshwork, n=6 technical replicates using four independent cell strains; dermal fibroblasts, n=3 technical replicates from three cell strains. * $p<0.05$; ** $p<0.005$ with one-way ANOVA.

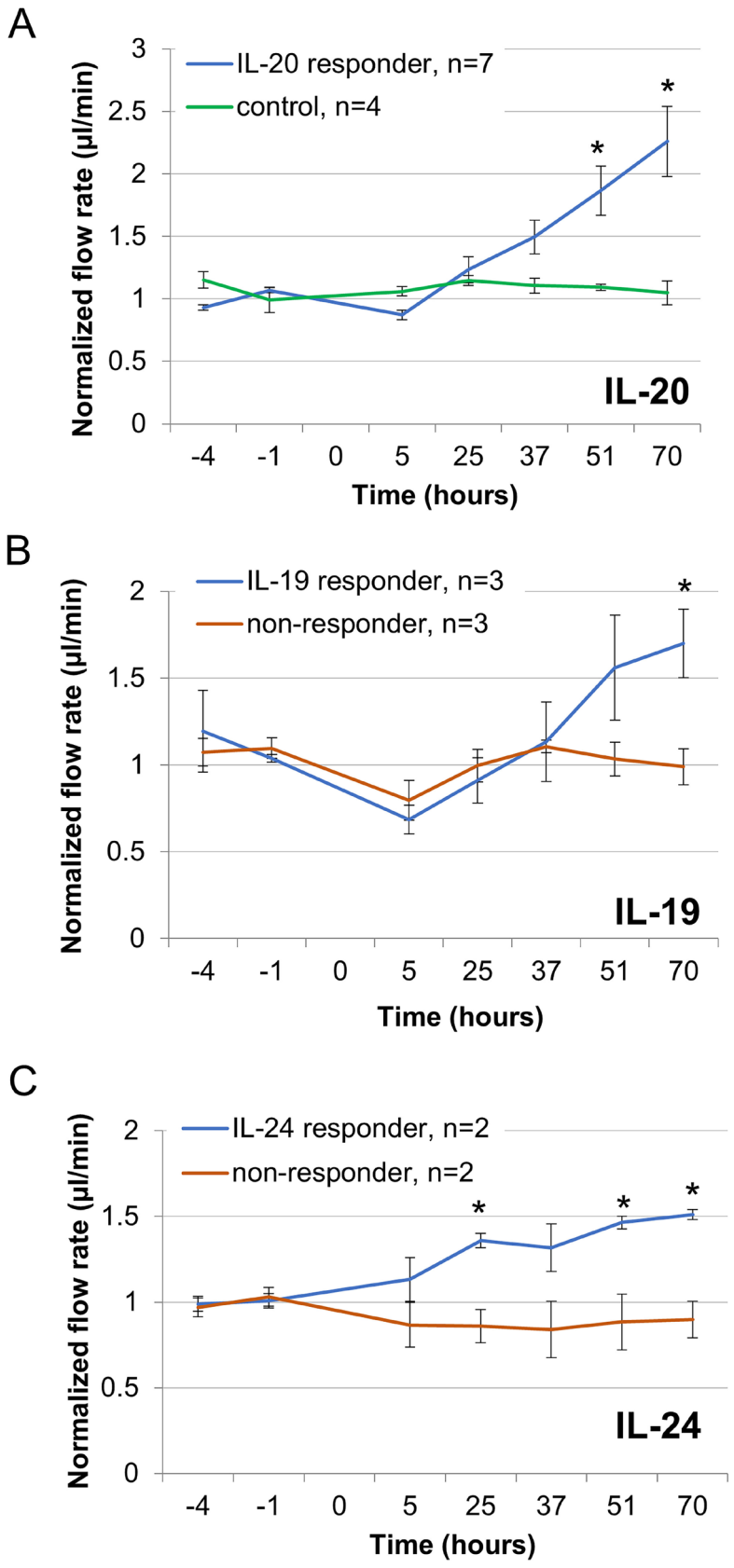

Figure 5. Human anterior segment perfusion culture. Outflow rates were measured in human anterior segments perfused with 100 ng/ml (**A**) interleukin-20 (IL-20), (**B**) IL-19, or (**C**) IL-24. Control in (**A**) is PBS as a vehicle. Cytokines were added at time point 0, and flow rates were measured for a further 70 h. The data show the average ± standard error of the mean. * $p<0.05$ and ** $p<0.01$ with ANOVA.

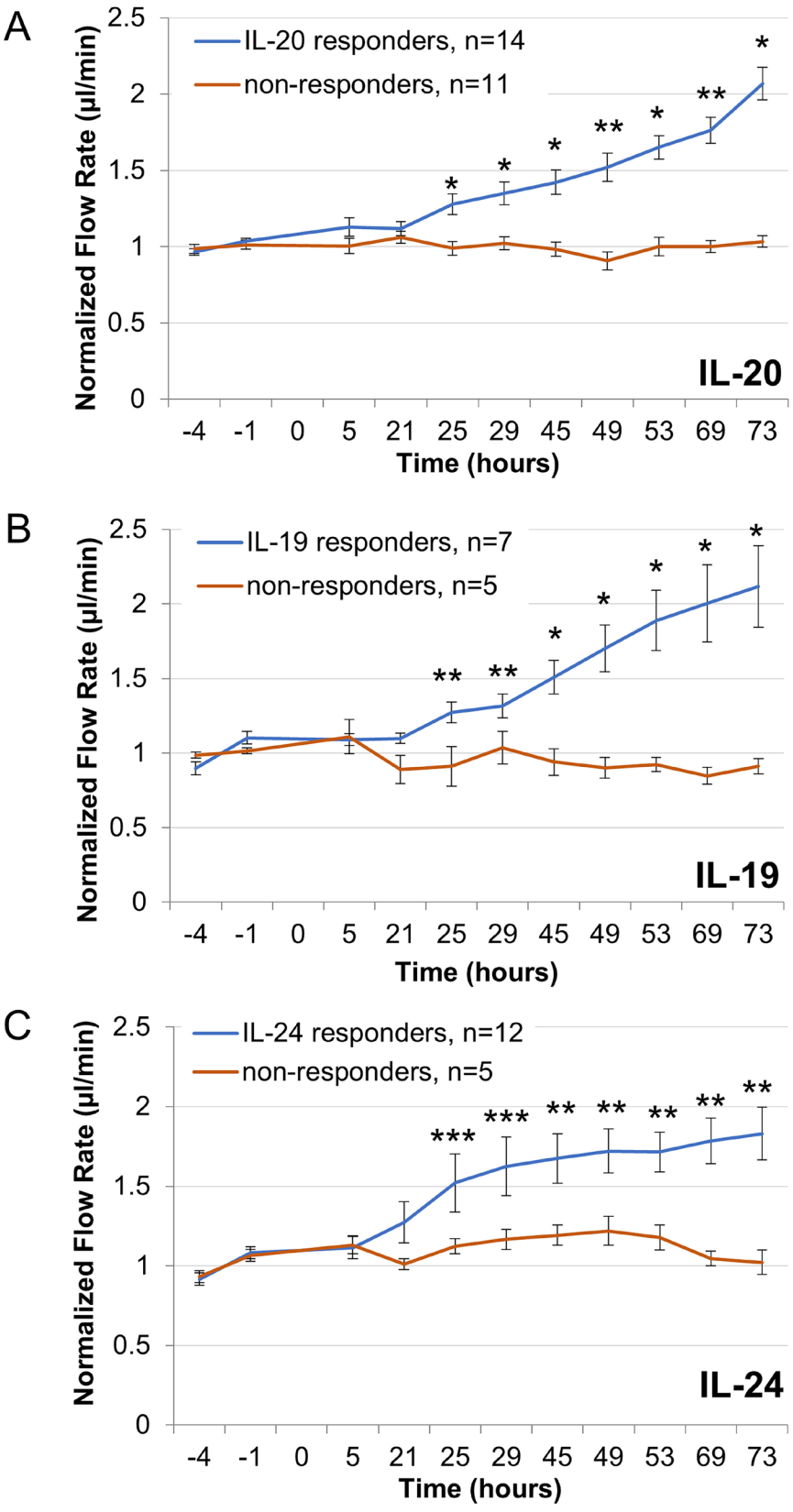

Figure 6. Porcine anterior segment perfusion culture. Outflow rates were measured in porcine anterior segments perfused with 100 ng/ml (**A**) interleukin-20 (IL-20) , (**B**) IL-19, or (**C**) IL-24. Cytokines were added at time point 0, and flow rates were measured for a further 73 h. The data show the average ± standard error of the mean. * p<0.001, ** p<0.01 and *** p<0.05 with ANOVA.

Table 1. Perfused human eye flow rates.

Eye Identifier	Treatment	Average flow rate before treatment	Flow rate @ 70 h	Fold-change	Responder	Non-responder
2016–1607						
OD	IL-20	2.85	4.62	1.62	X	-
OS	IL-20	3.30	5.41	1.64	X	-
2016–1615						
OD	IL-20	3.21	7.87	2.45	X	-
OS	IL-20	2.06	4.04	1.96	X	-
2016–1785						
OD	IL-20	1.71	5.08	2.97	X	-
2016–1780						
OS	IL-20	1.82	7.29	2.41	X	-
2016–1781						
OS	IL-20	2.49	6.0	2.41	X	-
2016–1705						
OD	IL-19	3.29	2.79	0.85	-	X
2016–1706						
OD	IL-19	1.30	1.55	1.19	-	X
OS	IL-24	3.63	2.88	0.79	-	X
2016–1707						
OD	IL-19	1.20	1.83	1.52	X	-
OS	IL-24	1.38	2.02	1.46	X	-
2016–1710						
OD	IL-19	7.10	6.62	0.93	-	X
OS	IL-24	2.91	2.99	1.03	-	X
2018–1630						
OD	IL-19	3.13	6.33	2.02	X	-
OS	IL-24	2.80	4.29	1.53	X	-
2018–1647						
OD	IL-19	2.13	3.12	1.46	X	-

All flow rates values are µl/min.

Ser727 phosphorylation in the dermal fibroblasts. Although this is the simplest interpretation, it remains possible that a lower number of spots in the Duolink assay may be due to intracellular dissociation of the heterodimeric complex following endocytosis. Future studies using overexpression of GFP-tagged IL-20RB will investigate the potential of IL-20R endocytosis. In addition, although cultured TM cells seem to utilize the Ser727 phosphorylation site of STAT-3, the significance of STAT phosphorylation in outflow experiments has not yet been tested. Nonetheless, these results may be important for other inflammatory diseases that involve IL-20 signaling, such as psoriasis, inflammatory bowel disease, liver inflammation, and rheumatoid arthritis [28,30]. Psoriasis is a chronic inflammatory disease of the skin with sharply demarcated, erythematous, and slightly elevated skin plaques covered by silvery white scales [46]. High levels of IL-19, IL-20, and the IL-20 type I receptor (IL-20RA–IL-20RB) are found in psoriatic skin [47-49]. The epidermis of IL-20 and IL-24 transgenic mice displays severe skin abnormalities resembling human psoriatic skin [48,50,51]. In contrast, IL-20RB knockout mice are born healthy with no apparent skin abnormalities, and are protected from stimuli that induce psoriasis [52,53]. The development of psoriasis in the skin, which can be triggered by overexpression of IL-20 cytokines, can be considered an uncontrolled wound-healing response, similar to acute reepithelialization [54]. The IL-20 subfamily participates in amplifying inflammatory responses, particularly during autoimmune and chronic inflammation, and alternatively, in anti-inflammatory responses, such as tissue protection and regeneration [28,30].

One of the most direct in vitro methods for studying the aqueous outflow pathway is to use perfusion-cultured anterior segments [55]. Therefore, we studied the effects of IL-19, IL-20, and IL-24 on outflow in human and porcine

Table 2. IL-20 perfused porcine eye flow rates.

Treatment	Average flow rate before treatment	Flow rate @ 73 h	Fold-change	Responder	Non-responder
IL-20	1.84	2.27	1.23	-	X
IL-20	1.07	1.66	1.54	X	-
IL-20	1.93	4.63	2.4	X	-
IL-20	2.19	3.875	1.76	X	-
IL-20	1.91	4.45	2.33	X	-
IL-20	1.82	3.33	1.83	X	-
IL-20	1.67	1.909	1.14	-	X
IL-20	1.87	1.69	0.90	-	X
IL-20	1.77	3.22	1.81	X	-
IL-20	2.93	2.93	1.00	-	X
IL-20	1.01	1.67	1.73	X	-
IL-20	3.43	2.95	0.86	-	X
IL-20	1.27	1.37	1.07	-	X
IL-20	1.85	1.83	0.98	-	X
IL-20	1.51	3.04	2.01	X	-
IL-20	1.42	2.29	1.60	X	-
IL-20	1.76	3.45	2.28	X	-
IL-20	1.36	1.16	0.85	-	X
IL-20	2.20	2.95	1.34	X	-
IL-20	1.03	1.06	1.02	-	X
IL-20	2.56	2.5	0.97	-	X
IL-20	1.39	2.41	1.72	X	-
IL-20	1.42	1.45	1.09	-	X

All flow rates values are µl/min. Shaded rows depict experiments that were run on the same date (n=5 experimental replicates).

Table 3. IL-19 perfused porcine eye flow rates.

Treatment	Average flow rate before treatment	Flow rate @ 73 h	Fold-change	Responder	Non-responder
IL-19	3.09	10.44	3.37	X	-
IL-19	2.45	2.11	0.86	-	X
IL-19	1.74	1.66	0.96	-	X
IL-19	1.66	1.66	1.0	-	X
IL-19	2.36	1.75	0.74	-	X
IL-19	1.23	2.95	2.4	X	-
IL-19	1.49	3.125	2.08	X	-
IL-19	1.01	1.25	1.31	X	-
IL-19	2.53	4.41	1.74	X	-
IL-19	5.55	5.58	1.00	-	X
IL-19	2.68	6.79	2.52	X	-
IL-19	3.22	4.45	1.38	X	-

All flow rates values are µl/min. Shaded rows depict experiments that were run on the same date (n=4 experimental replicates).

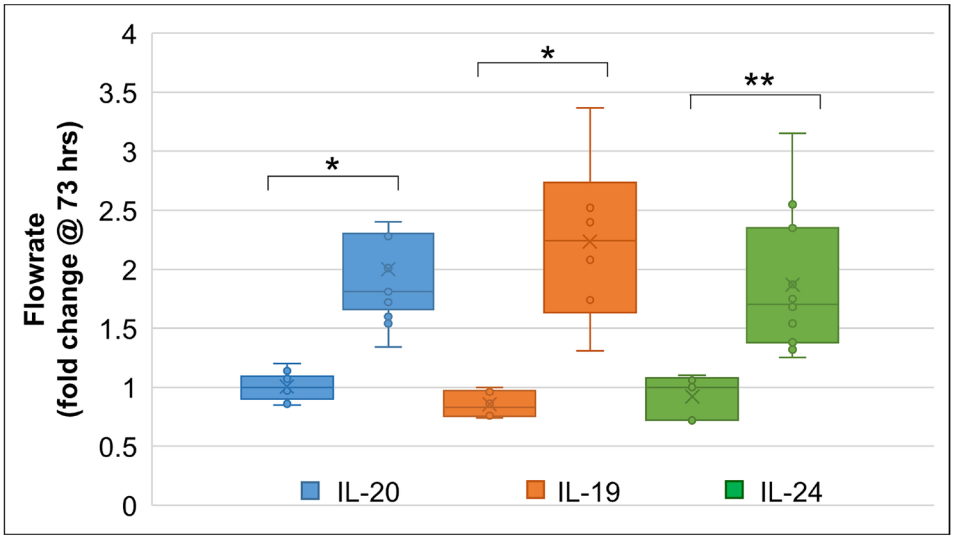

Figure 7. Analysis of the porcine flow rate data at 73 h. Comparison of non-responders and responders to interleukin-20 (IL-20) IL-20, IL-19, and IL-24. Error bars are the standard error of the mean, the cross is the mean, and the line across the center of the box is the median. The outlier data point for IL-20 is not shown. * p<0.001, ** p<0.01.

eye models. The results of the experiments revealed some anterior segments were cytokine "responders," and a nearly equal number were "non-responders." This was not due to cytokine batch differences, because porcine perfusion experiments run on the same day showed that some eyes responded while others did not (Table 2, Table 3, and Table 4). We also hypothesized that human recombinant cytokines might not be recognized by porcine receptors. However, the comparison of the human and porcine IL-20 receptor amino acid sequences showed all residues that made direct contact with the cytokines were conserved. Thus, we conclude that porcine IL-20 receptors have the capacity to bind and respond to human IL-20 cytokines. Analyzing the human data shows that in certain individuals, both eyes of a pair did not respond

Table 4. IL-24 perfused porcine eye flow rates.

Treatment	Average flow rate before treatment	Flow rate @ 73 h	Fold-change	Responder	Non-responder
IL-24	1.71	2	1.17	-	X
IL-24	1.90	2.11	1.10	-	X
IL-24	1.96	2.75	1.39	X	-
IL-24	1.42	2.41	1.70	X	-
IL-24	1.51	2.33	1.54	X	-
IL-24	3.68	3.87	1.05	-	X
IL-24	2.41	1.75	0.72	-	X
IL-24	1.76	3.08	1.75	X	-
IL-24	1.12	2.8	2.55	X	-
IL-24	3.42	8.08	2.35	X	-
IL-24	3.53	4.875	1.38	X	-
IL-24	4.47	7.54	1.68	X	-
IL-24	1.87	5.91	3.15	X	-
IL-24	2.51	4.71	1.87	X	-
IL-24	1.92	2.54	1.32	X	-
IL-24	2.25	2.83	1.25	X	-
IL-24	2.94	3.12	1.06	-	X

All flow rates values are µl/min. Shaded rows depict experiments that were run on the same date (n=5 experimental replicates).

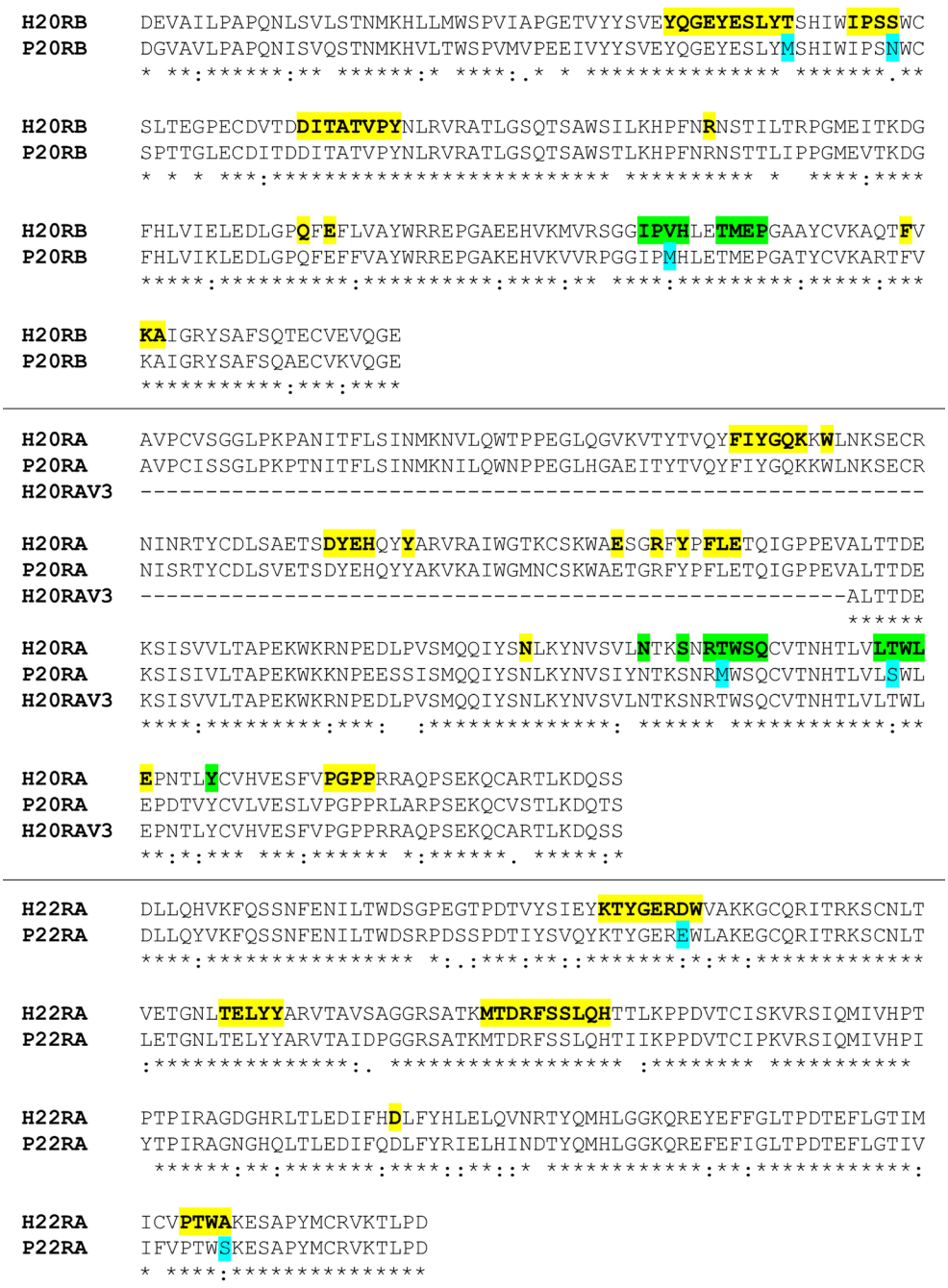

Figure 8. Amino acid sequence alignments of human and porcine IL-20 receptors. Receptor-cytokine (bold/yellow) and receptor-receptor (bold/green) contact residues are highlighted. Residue changes in the porcine receptors are highlighted in cyan. Contact residues are based on the crystal structure of the interleukin-20 (IL-20)–IL-20RA–IL-20RB complex (pdbid=4doh). H, human; P, porcine.

demonstrating congruence in response within an individual (Table 1). All eyes were screened routinely with hematoxylin and eosin staining of sections, and all TM tissue contained cells (not shown). However, it remains possible that there were lower cell numbers in the non-responding eyes, thus lowering the potential to bind and propagate cytokine signals. However, one of the non-responders (2016–1705) was 42 years old at the time of death, and was unlikely to have reduced cell loss, which is more often seen in elderly TM tissue [56]. Thus, the data suggest that certain individuals are more responsive to IL-20 family cytokine signals than others.

This study is not the first to report differences in response to treatments. Interestingly, "responders" and "non-responders" have also been described for glucocorticoids, such as dexamethasone. Glucocorticoids can induce ocular hypertension in approximately 40% of the general population, and at a much higher rate in patients with glaucoma [18,57,58]. Glucocorticoids induce their effects via the glucocorticoid receptor (GR), which undergoes alternative splicing to produce GRα and GRβ [59]. The GRβ isoform is a dominant negative inhibitor of GRα function, and their relative ratio regulates glucocorticoid responsiveness in TM cells and in mice [18,60].

In conclusion, the present results demonstrated that ocular TM cells express all IL-20 receptors, and predominantly signal through the type I receptor, which can propagate signals from IL-20, IL-19, and IL-24 cytokines. Finally, the outflow results suggest that responses to IL-20 cytokines are variable. As a result, some individuals are unable to alter outflow rates when exposed to IL-20 cytokines. Thus, these results may explain why some individuals are more susceptible to developing elevated IOP in response to inflammation.

APPENDIX 1. SUMMARY OF THE DONORS FOR THE CELL STRAINS.

To access the data, click or select the words "Appendix 1."

APPENDIX 2. PCR PRIMERS USED TO DETERMINE ALTERNATIVE SPLICING OF IL-20RA.

To access the data, click or select the words "Appendix 2."

APPENDIX 3. NEGATIVE CONTROL FOR FIGURE 3 WITH REPLACEMENT OF PRIMARY ANTIBODIES BY PBS

A representative confocal image of a negative control of the Duolink assay, where primary antibodies were substituted with PBS. Scale bar=20 µm. To access the data, click or select the words "Appendix 3."

ACKNOWLEDGMENTS

The authors would like to thank Lions VisionGift, Portland, OR for their help in the procurement of human eye cadaver tissue. This work was supported by NIH/NEI grants R21EY027079 (MKW), R01EY11650 (MKW) and P30EY010572 (Casey Eye Institute Core facility grant) and an unrestricted grant to the Casey Eye Institute from Research to Prevent Blindness, New York, NY.

REFERENCES

1. Tham YC, Li X, Wong TY, Quigley HA, Aung T, Cheng CY. Global prevalence of glaucoma and projections of glaucoma burden through 2040: a systematic review and meta-analysis. Ophthalmology 2014; 121:2081-90. [PMID: 24974815].
2. Rein DB, Zhang P, Wirth KE, Lee PP, Hoerger TJ, McCall N, Klein R, Tielsch JM, Vijan S, Saaddine J. The economic burden of major adult visual disorders in the United States. Arch Ophthalmol 2006; 124:1754-60. [PMID: 17159036].
3. Foster PJ, Buhrmann R, Quigley HA, Johnson GJ. The definition and classification of glaucoma in prevalence surveys. Br J Ophthalmol 2002; 86:238-42. [PMID: 11815354].
4. Malihi M, Moura Filho ER, Hodge DO, Sit AJ. Long-term trends in glaucoma-related blindness in Olmsted County, Minnesota. Ophthalmology 2014; 121:134-41. [PMID: 24823760].
5. Tielsch JM, Katz J, Singh K, Quigley HA, Gottsch JD, Javitt J, Sommer A. A population-based evaluation of glaucoma screening: the Baltimore Eye Survey. Am J Epidemiol 1991; 134:1102-10. [PMID: 1746520].
6. Mozaffarieh M, Fraenkl S, Konieczka K, Flammer J. Targeted preventive measures and advanced approaches in personalised treatment of glaucoma neuropathy. EPMA J 2010; 1:229-35. [PMID: 23199061].
7. Stamer WD, Acott TS. Current understanding of conventional outflow dysfunction in glaucoma. Curr Opin Ophthalmol 2012; 23:135-43. [PMID: 22262082].
8. Quigley HA. Glaucoma. Lancet 2011; 377:1367-77. [PMID: 21453963].
9. Kwon YH, Fingert JH, Kuehn MH, Alward WL. Primary open-angle glaucoma. N Engl J Med 2009; 360:1113-24. [PMID: 19279343].
10. Tian K, Shibata-Germanos S, Pahlitzsch M, Cordeiro MF. Current perspective of neuroprotection and glaucoma. Clin Ophthalmol 2015; 9:2109-18. [PMID: 26635467].
11. Keller KE, Yang YF, Sun YY, Sykes R, Gaudette ND, Samples JR, Acott TS, Wirtz MK. Interleukin-20 receptor expression in the trabecular meshwork and its implication in glaucoma. J Ocul Pharmacol Ther 2014; 30:267-76. [PMID: 24455976].
12. Wang N, Chintala SK, Fini ME, Schuman JS. Activation of a tissue-specific stress response in the aqueous outflow pathway of the eye defines the glaucoma disease phenotype. Nat Med 2001; 7:304-9. [PMID: 11231628].
13. Soto I, Howell GR. The complex role of neuroinflammation in glaucoma. Cold Spring Harb Perspect Med 2014; 4:4-[PMID: 24993677].
14. McKinnon SJ. The cell and molecular biology of glaucoma: common neurodegenerative pathways and relevance to glaucoma. Invest Ophthalmol Vis Sci 2012; 53:2485-7. [PMID: 22562847].
15. Krizaj D, Ryskamp DA, Tian N, Tezel G, Mitchell CH, Slepak VZ, Shestopalov VI. From mechanosensitivity to

inflammatory responses: new players in the pathology of glaucoma. Curr Eye Res 2014; 39:105-19. [PMID: 24144321].

16. Stern JJ. Acute glaucoma during cortisone therapy. Am J Ophthalmol 1953; 36:389-90. [PMID: 13030647].

17. Francois J. Cortisone et tension oculaire. Ann Ocul (Paris) 1954; 187:805-16. [PMID: 13218439].

18. Fini ME, Schwartz SG, Gao X, Jeong S, Patel N, Itakura T, Price MO, Price FW Jr, Varma R, Stamer WD. Steroid-induced ocular hypertension/glaucoma: Focus on pharmacogenomics and implications for precision medicine. Prog Retin Eye Res 2017; 56:58-83. [PMID: 27666015].

19. Becker B, Mills DW. Elevated Intraocular Pressure Following Corticosteroid Eye Drops. JAMA 1963; 185:884-6. [PMID: 14043096].

20. Armaly MF, Becker B. Intraocular pressure response to topical corticosteroids. Fed Proc 1965; 24:1274-8. [PMID: 5853148].

21. Becker B. Intraocular Pressure Response to Topical Corticosteroids. Invest Ophthalmol 1965; 4:198-205. [PMID: 14283013].

22. Pasutto F, Keller KE, Weisschuh N, Sticht H, Samples JR, Yang YF, Zenkel M, Schlotzer-Schrehardt U, Mardin CY, Frezzotti P, Edmunds B, Kramer PL, Gramer E, Reis A, Acott TS, Wirtz MK. Variants in ASB10 are associated with open-angle glaucoma. Hum Mol Genet 2012; 21:1336-49. [PMID: 22156576].

23. Wirtz MK, Samples JR, Kramer PL, Rust K, Topinka JR, Yount J, Koler RD, Acott TS. Mapping a gene for adult-onset primary open-angle glaucoma to chromosome 3q. Am J Hum Genet 1997; 60:296-304. [PMID: 9012402].

24. Wirtz MK, Samples JR, Rust K, Lie J, Nordling L, Schilling K, Acott TS, Kramer PL. GLC1F, a new primary open-angle glaucoma locus, maps to 7q35-q36. Arch Ophthalmol 1999; 117:237-41. [PMID: 10037570].

25. Monemi S, Spaeth G, DaSilva A, Popinchalk S, Ilitchev E, Liebmann J, Ritch R, Heon E, Crick RP, Child A, Sarfarazi M. Identification of a novel adult-onset primary open-angle glaucoma (POAG) gene on 5q22.1. Hum Mol Genet 2005; 14:725-33. [PMID: 15677485].

26. Liu Y, Allingham RR. Major review: Molecular genetics of primary open-angle glaucoma. Exp Eye Res 2017; 160:62-84. [PMID: 28499933].

27. Logsdon NJ, Deshpande A, Harris BD, Rajashankar KR, Walter MR. Structural basis for receptor sharing and activation by interleukin-20 receptor-2 (IL-20R2) binding cytokines. Proc Natl Acad Sci USA 2012; 109:12704-9. [PMID: 22802649].

28. Rutz S, Wang X, Ouyang W. The IL-20 subfamily of cytokines–from host defence to tissue homeostasis. Nat Rev Immunol 2014; 14:783-95. [PMID: 25421700].

29. Hsu YH, Chang MS. IL-20 in rheumatoid arthritis. Drug Discov Today 2017; 22:960-4. [PMID: 26297177].

30. Wegenka UM. IL-20: biological functions mediated through two types of receptor complexes. Cytokine Growth Factor Rev 2010; 21:353-63. [PMID: 20864382].

31. Ouyang W, Rutz S, Crellin NK, Valdez PA, Hymowitz SG. Regulation and functions of the IL-10 family of cytokines in inflammation and disease. Annu Rev Immunol 2011; 29:71-109. [PMID: 21166540].

32. Jiang H, Lin JJ, Su ZZ, Goldstein NI, Fisher PB. Subtraction hybridization identifies a novel melanoma differentiation associated gene, mda-7, modulated during human melanoma differentiation, growth and progression. Oncogene 1995; 11:2477-86. [PMID: 8545104].

33. Keller KE, Bhattacharya SK, Borras T, Brunner TM, Chansangpetch S, Clark AF, Dismuke WM, Du Y, Elliott MH, Ethier CR, Faralli JA, Freddo TF, Fuchshofer R, Giovingo M, Gong H, Gonzalez P, Huang A, Johnstone MA, Kaufman PL, Kelley MJ, Knepper PA, Kopczynski CC, Kuchtey JG, Kuchtey RW, Kuehn MH, Lieberman RL, Lin SC, Liton P, Liu Y, Lutjen-Drecoll E, Mao W, Masis-Solano M, McDonnell F, McDowell CM, Overby DR, Pattabiraman PP, Raghunathan VK, Rao PV, Rhee DJ, Chowdhury UR, Russell P, Samples JR, Schwartz D, Stubbs EB, Tamm ER, Tan JC, Toris CB, Torrejon KY, Vranka JA, Wirtz MK, Yorio T, Zhang J, Zode GS, Fautsch MP, Peters DM, Acott TS, Stamer WD. Consensus recommendations for trabecular meshwork cell isolation, characterization and culture. Exp Eye Res 2018; 171:164-73. [PMID: 29526795].

34. Erickson-Lamy K, Rohen JW, Grant WM. Outflow facility studies in the perfused human ocular anterior segment. Exp Eye Res 1991; 52:723-31. [PMID: 1855546].

35. Keller KE, Bradley JM, Kelley MJ, Acott TS. Effects of modifiers of glycosaminoglycan biosynthesis on outflow facility in perfusion culture. Invest Ophthalmol Vis Sci 2008; 49:2495-505. [PMID: 18515587].

36. Sievers F, Higgins DG. Clustal Omega, accurate alignment of very large numbers of sequences. Methods Mol Biol 2014; 1079:105-16. [PMID: 24170397].

37. Krissinel E, Henrick K. Inference of macromolecular assemblies from crystalline state. J Mol Biol 2007; 372:774-97. [PMID: 17681537].

38. Blokzijl A, Friedman M, Ponten F, Landegren U. Profiling protein expression and interactions: proximity ligation as a tool for personalized medicine. J Intern Med 2010; 268:232-45. [PMID: 20695973].

39. Lejeune D, Dumoutier L, Constantinescu S, Kruijer W, Schuringa JJ, Renauld JC. Interleukin-22 (IL-22) activates the JAK/STAT, ERK, JNK, and p38 MAP kinase pathways in a rat hepatoma cell line. Pathways that are shared with and distinct from IL-10. J Biol Chem 2002; 277:33676-82. [PMID: 12087100].

40. Zhu X, Wen Z, Xu LZ, Darnell JE Jr. Stat1 serine phosphorylation occurs independently of tyrosine phosphorylation and requires an activated Jak2 kinase. Mol Cell Biol 1997; 17:6618-23. [PMID: 9343425].

41. Hillmer EJ, Zhang H, Li HS, Watowich SS. STAT3 signaling in immunity. Cytokine Growth Factor Rev 2016; 31:1-15. [PMID: 27185365].

42. Able AA, Burrell JA, Stephens JM. STAT5-Interacting Proteins: A Synopsis of Proteins that Regulate STAT5 Activity. Biology (Basel) 2017; 6:6-[PMID: 28287479].

43. Johnson DH, Tschumper RC. The effect of organ culture on human trabecular meshwork. Exp Eye Res 1989; 49:113-27. [PMID: 2759186].

44. Johnson DH, Tschumper RC. Human trabecular meshwork organ culture. A new method. Invest Ophthalmol Vis Sci 1987; 28:945-53. [PMID: 3583633].

45. Grant WM. Experimental aqueous perfusion in enucleated human eyes. Arch Ophthalmol 1963; 69:783-801. [PMID: 13949877].

46. Boehncke WH, Schon MP. Psoriasis. Lancet 2015; 386:983-94. [PMID: 26025581].

47. Li HH, Lin YC, Chen PJ, Hsiao CH, Lee JY, Chen WC, Tzung TY, Wu JC, Chang MS. Interleukin-19 upregulates keratinocyte growth factor and is associated with psoriasis. Br J Dermatol 2005; 153:591-5. [PMID: 16120148].

48. Blumberg H, Conklin D, Xu WF, Grossmann A, Brender T, Carollo S, Eagan M, Foster D, Haldeman BA, Hammond A, Haugen H, Jelinek L, Kelly JD, Madden K, Maurer MF, Parrish-Novak J, Prunkard D, Sexson S, Sprecher C, Waggie K, West J, Whitmore TE, Yao L, Kuechle MK, Dale BA, Chandrasekher YA. Interleukin 20: discovery, receptor identification, and role in epidermal function. Cell 2001; 104:9-19. [PMID: 11163236].

49. Otkjaer K, Kragballe K, Funding AT, Clausen JT, Noerby PL, Steiniche T, Iversen L. The dynamics of gene expression of interleukin-19 and interleukin-20 and their receptors in psoriasis. Br J Dermatol 2005; 153:911-8. [PMID: 16225599].

50. He M, Liang P. IL-24 transgenic mice: in vivo evidence of overlapping functions for IL-20, IL-22, and IL-24 in the epidermis. J Immunol 2010; 184:1793-8. [PMID: 20061404].

51. Liu L, Ding C, Zeng W, Heuer JG, Tetreault JW, Noblitt TW, Hangoc G, Cooper S, Brune KA, Sharma G, Fox N, Rowlinson SW, Rogers DP, Witcher DR, Lambooy PK, Wroblewski VJ, Miller JR, Broxmeyer HE. Selective enhancement of multipotential hematopoietic progenitors in vitro and in vivo by IL-20. Blood 2003; 102:3206-9. [PMID: 12855566].

52. Chan JR, Blumenschein W, Murphy E, Diveu C, Wiekowski M, Abbondanzo S, Lucian L, Geissler R, Brodie S, Kimball AB, Gorman DM, Smith K, de Waal Malefyt R, Kastelein RA, McClanahan TK, Bowman EP. IL-23 stimulates epidermal hyperplasia via TNF and IL-20R2-dependent mechanisms with implications for psoriasis pathogenesis. J Exp Med 2006; 203:2577-87. [PMID: 17074928].

53. Wahl C, Muller W, Leithauser F, Adler G, Oswald F, Reimann J, Schirmbeck R, Seier A, Weiss JM, Prochnow B, Wegenka UM. IL-20 receptor 2 signaling down-regulates antigen-specific T cell responses. J Immunol 2009; 182:802-10. [PMID: 19124723].

54. Sano S, Chan KS, Carbajal S, Clifford J, Peavey M, Kiguchi K, Itami S, Nickoloff BJ, DiGiovanni J. Stat3 links activated keratinocytes and immunocytes required for development of psoriasis in a novel transgenic mouse model. Nat Med 2005; 11:43-9. [PMID: 15592573].

55. Clark AF, Wilson K, de Kater AW, Allingham RR, McCartney MD. Dexamethasone-induced ocular hypertension in perfusion-cultured human eyes. Invest Ophthalmol Vis Sci 1995; 36:478-89. [PMID: 7843916].

56. Alvarado J, Murphy C, Polansky J, Juster R. Age-related changes in trabecular meshwork cellularity. Invest Ophthalmol Vis Sci 1981; 21:714-27. [PMID: 7298275].

57. Clark AF, Wordinger RJ. The role of steroids in outflow resistance. Exp Eye Res 2009; 88:752-9. [PMID: 18977348].

58. Jones R 3rd, Rhee DJ. Corticosteroid-induced ocular hypertension and glaucoma: a brief review and update of the literature. Curr Opin Ophthalmol 2006; 17:163-7. [PMID: 16552251].

59. Jain A, Wordinger RJ, Yorio T, Clark AF. Role of the alternatively spliced glucocorticoid receptor isoform GRbeta in steroid responsiveness and glaucoma. J Ocul Pharmacol Ther 2014; 30:121-7. [PMID: 24506296].

60. Patel GC, Liu Y, Millar JC, Clark AF. Glucocorticoid receptor GRbeta regulates glucocorticoid-induced ocular hypertension in mice. Sci Rep 2018; 8:862-[PMID: 29339763].

61. Parrish-Novak J, Xu W, Brender T, Yao L, Jones C, West J, Brandt C, Jelinek L, Madden K, McKernan PA, Foster DC, Jaspers S, Chandrasekher YA. Interleukins 19, 20, and 24 signal through two distinct receptor complexes. Differences in receptor-ligand interactions mediate unique biological functions. J Biol Chem 2002; 277:47517-23. [PMID: 12351624].

62. Yan H, Krishnan K, Lim JT, Contillo LG, Krolewski JJ. Molecular characterization of an alpha interferon receptor 1 subunit (IFNaR1) domain required for TYK2 binding and signal transduction. Mol Cell Biol 1996; 16:2074-82. [PMID: 8628273].

63. Dumoutier L, Leemans C, Lejeune D, Kotenko SV, Renauld JC. Cutting edge: STAT activation by IL-19, IL-20 and mda-7 through IL-20 receptor complexes of two types. J Immunol 2001; 167:3545-9. [PMID: 11564763].

Articles are provided courtesy of Emory University and the Zhongshan Ophthalmic Center, Sun Yat-sen University, P.R. China. The print version of this article was created on 27 April 2019. This reflects all typographical corrections and errata to the article through that date. Details of any changes may be found in the online version of the article.